Strategic Deconfliction of Small Unmanned Aircraft Using Operational Volume Blocks at Crossing Waypoints

Priyank Pradeep *
Universities Space Research Association, Moffett Field, CA, 94035, USA.

Alexey A. Munishkin †, Krishna M. Kalyanam ‡, and Heinz Erzberger §
NASA Ames Research Center, Moffett Field, CA, 94035, USA.

In this research, first, analytical case studies are performed to understand the parameters on which the minimum temporal separation between unmanned aircraft at crossing waypoints is dependent for enabling strategic deconfliction. The analytical expressions show that the minimum temporal separation is a function of the length and width of operational volume blocks, the relative positions of the active operational volume blocks, groundspeed of unmanned aircraft, and the incoming crossing angle. Next, the parametric study shows that the impact of the incoming crossing angle on the minimum temporal separation at a crossing waypoint increases with an increase in the width of the operational volume blocks. Finally, simulation studies are performed to understand the impact of operational volume block sizing, on-demand departure rate, minimum departure time separation, and the incoming crossing angle on the average ground delay of unmanned aircraft traveling on two routes with a single crossing waypoint and identical on-demand departure rate. Each unmanned aircraft's estimated time of arrival at a crossing waypoint is adjusted by introducing a ground delay in departure time; no other controls (e.g., speed adjustments) are applied for strategic deconfliction. Simulation studies show that the impact of the minimum temporal separation at a crossing waypoint on the average ground delay of flights is negligible if the minimum departure time separation is at least two times the minimum temporal separation. Therefore, with an increase in minimum departure time separation at a depot, the impact of increased length of operational volume blocks enclosing the crossing waypoint on the ground delay is offset to an extent.

I. Introduction

Small unmanned aircraft systems (UAS), with the mass of unmanned aircraft (UA) less than 55 lbs, are envisioned to provide socio-economic benefits to the public by revolutionizing operations related to small package delivery, precision agriculture scouting, surveillance, supporting first responders, and inspection of critical infrastructure like railroads and bridges [1, 2]. In general, the commercial small UAS consists of four main components [3]: i) UA, ii) ground-based controller, iii) command and control (C2) system - to link the UA with the ground controller, and iv) payload (package for delivery). These UA are anticipated to operate: i) much closer to each other (higher traffic density) than conventional aircraft, ii) exclusively in low-altitude airspace, i.e., less than 400 ft above ground level (AGL) [2], and iii) beyond visual line of sight (BVLOS) in the National Airspace System (NAS) [3, 4]. UAS traffic management (UTM) has been envisioned to have multiple layers of separation assurance to ensure the safe operations of small UAS, from strategic flight planning and management to tactical aircraft and obstacle avoidance capabilities [3]. The objective of strategic deconfliction is to minimize the likelihood of airborne conflicts between UAS operations by adjusting the departure times of UAS [4]. On the other hand, an en-route tactical separation management service is also key to safety due to uncertainty in flight trajectories and environmental conditions (e.g., wind) [5, 6].

In the UTM ecosystem, UAS operators planning to fly BVLOS are required to share operational intent with other UAS operators/airspace users via the UAS Supplier Service (USS) network [3, 4]. The operational intent includes a sequence of 4D (spatiotemporal) operational volume blocks that make up the intended flight profile [3, 7, 8]. In this research, each operational volume block is assumed to be fixed in space and has specified entry and exit times for the

*Aerospace Engineer, Universities Space Research Association, NASA Ames Research Center, AIAA Senior Member.
†Pathways Intern, Aviation Systems Division, NASA Ames Research Center, AIAA Member.
‡Aerospace Research Engineer, Aviation Systems Division, NASA Ames Research Center, AIAA Senior Member.
§Ames Associate, Aviation Systems Division, NASA Ames Research Center, AIAA Fellow.

UAS operator's UA per NASA and the FAA's UTM concept of operations [3, 4, 7]. In the operation planning phase, prior to departure, the UAS operator or operator's USS checks the operational volume blocks against other operations for any 4D conflicts. If any spatiotemporal overlapping of operational volume blocks is detected, then negotiation and replanning of the operational intent of the UAS are performed [3, 9]. As shown in Figure 1, given the 400 ft AGL upper bound constraint for the cruise altitude of small UAS operations [2], whenever there is a spatial overlapping of two operational intents of different UAS operators, for example, at a crossing waypoint, then deconfliction of overlapping operational volume blocks can be performed via temporal separation at the waypoint [3].

In general, the complexity of a traffic scenario increases in the presence of crossing and merging waypoints in the network [10, 11]. Lauderdale et al. [6] used a point mass model for electric vertical takeoff and landing (eVTOL) aircraft to show that the minimum temporal separation to avoid conflict detection by a tactical separation assurance algorithm at a crossing waypoint is a complex function of crossing geometry, aircraft states, look-ahead time of separation assurance service, and wind characteristics. In the current research, analytical studies are performed using specific case studies to understand the impact of the operational volume block sizing (length and width), UA groundspeed, incoming crossing angle of routes, and relative positions of operational volume blocks on the required minimum temporal separation at a crossing waypoint for conflict-free flights.

The rest of the paper is organized as follows. In section II, analytical case studies are performed to understand the strategic deconfliction of operational volume blocks at crossing waypoints. In Section III, simulation studies are performed to understand the impact of operational volume block sizing, on-demand departure rate (Poisson distribution), minimum departure time separation, and incoming crossing angle on the average ground delay of UA flying on two routes with a single crossing waypoint (intersection) and identical departure rate. Finally, in Section IV, the main findings from this research study are summarized.

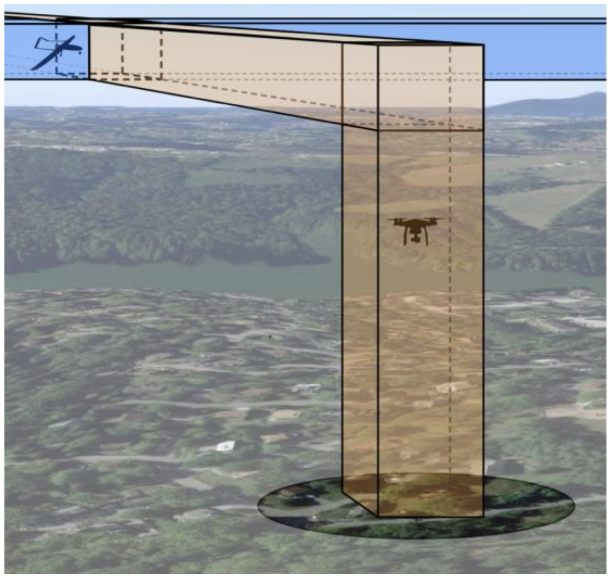

Fig. 1 Active Operational Volume Blocks (OVBs) Deconflicted via Temporal Separation [3]

II. Analytical Studies of Strategic Deconfliction at Crossing Waypoints

This research assumes the following regarding the operational intent (OI) and operational volume blocks (OVBs) based on NASA and the FAA's concept of operations for UTM [1, 3, 4, 7]:

- An operational intent of a small UAS consists of a sequence of 4D (spatiotemporal) operational volume blocks that make up the intended flight profile.
- An operational intent is wrapped around a notional flight path through the center of the operational volume blocks based on the expected groundspeed of the small UAS.
- A crossing waypoint is a point of intersection between two nominal flight paths.
- Operational volume blocks are fixed volumes in space that are active for a finite time. Therefore, they have specified entry and exit times for the small UA as shown in Figure 2.

- Operational volume blocks are right rectangular prisms in shape near crossing waypoints.
- A small UA is supposed to be inside the active (one) operational volume block at a specific time for conformance and conflict-free flight.
- Spatiotemporal overlapping of two active operational volume blocks of different UAS operators is considered as a conflict.

Note that a UAS operator may not necessarily know the exact position, direction (heading and course), groundspeed and airspeed information of a flight of another UAS operator in real-time. However, a small UA's entry and exit times in the operational volume block are published, ensuring conflict-free flights.

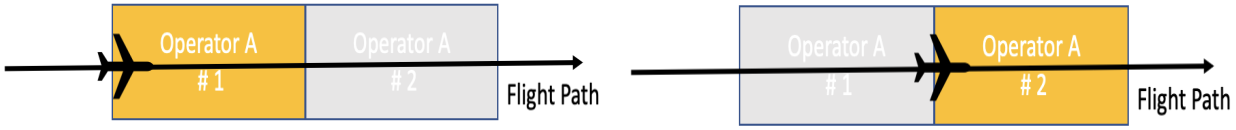

(a) Lateral view of active operational volume block # 1 **(b) Lateral view of active operational volume block # 2**

Fig. 2 Activation and Deactivation of Operational Volume Block (OVB) as an Unmanned Aircraft Enters and Exits

A. Analytical Case Studies - Strategic Deconfliction at Crossing Waypoints

Consider two routes crossing at the same altitude with one route for UAS operator A and the other route for UAS operator B, as shown in Figures 3, 4, 5 and 6. This research analyzes the minimum temporal separation at a crossing waypoint between i) the operational volume blocks of UAS operator A and UAS operator B such that there is no spatiotemporal overlapping of active operational volume blocks and ii) the UA of operator A and operational volume blocks of UAS operator B such that the UA of one UAS operator does not enter the active operational volume block of the other UAS operator in the vicinity of the crossing waypoint. Three operational volume blocks have been considered per operator for four case studies as shown in Figures 3, 4, 5, and 6 for the analyses. The four specific case studies were chosen to understand the impact of operational volume block sizing, on-demand departure rate (Poisson distribution), minimum departure time separation, and incoming crossing angle on the required minimum temporal separation between a UA of one operator (A) and active operational blocks of another operator (B) for strategic deconfliction. The strategic deconfliction between a UA of one UAS operator and active operational volume blocks of another UAS operator is considered equivalent to the strategic deconfliction between two UA, given the exact position and velocity of one UAS operator's UA inside the active operational volume block may be unknown to the other UAS operator in real-time. For a given UAS operator (A or B), the length (l_A or l_B) and width (W_A or W_B) of operational volume blocks are assumed to be constant. Three operational volume blocks per UAS operator are considered for each case study. In case study I and case study II, though the obtuse incoming crossing angle is the same, the relative positions of operational volume blocks are different. A similar analysis is performed for an acute incoming crossing angle in case studies III and IV.

1. Case Study I - Incoming Crossing at Obtuse Angle (90 deg < θ < 180 deg)

As shown in Subfigure 3a active operational volume block (# 1) of UAS operator B has a leading edge so close to the crossing waypoint such that the active operational volume block (# 1) of UAS operator A can not enclose the crossing waypoint. Similarly, as shown in Subfigure 3b, since the active operational volume block (# 2) of UAS operator B has enclosed the crossing waypoint, therefore, the active operational volume block (# 2) of UAS operator A can not enclose the crossing waypoint. In this case study, the point on the leading edge of UAS operator A's operational volume block (# 2) touches the side of UAS operator B's operational volume block (# 2). Hence the temporal separation at the crossing waypoint for strategic deconfliction of active operational volume blocks of UAS operators A and B is as follows:

$$\Delta T_{OVB-OVB} = \frac{2l_B}{V_B} \tag{1}$$

Temporal separation between the estimated time of arrival of the UA of UAS operator A at the crossing waypoint and the activation time of the first active operational volume block (# 1) of UAS operator B blocking the crossing waypoint

Table 1 Definition of Terms Used in Temporal Separation Equations

Term	Definition
$\Delta T_{OVB-OVB}$	Temporal separation between activation time of the operational volume block (# 3) of UAS operator A (enclosing the crossing waypoint) and the activation time of the first active operational volume block (# 1) of UAS operator B blocking the crossing waypoint.
ΔT_{UA-OVB}	Temporal separation between the estimated time of arrival of the UA of UAS operator A at the crossing waypoint and the activation time of the first active operational volume block (# 1) of UAS operator B blocking the crossing waypoint.
d_{TE-WPT}	Great-circle distance between the crossing waypoint and the trailing edge of the active operational volume block (enclosing the crossing waypoint) of UAS operator A.
V_A, V_B	Groundspeed of the UA of UAS operator A or B (assumed to be constant).
l_A, l_B	Length of the active operational volume block of UAS operator A or B.
W_A, W_B	Width of the active operational volume block of UAS operator A or B.
θ	Incoming crossing angle at the waypoint.

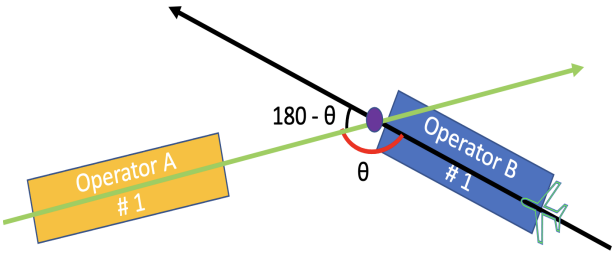

(a) Initially, operational volume blocks # 1 of UAS operators are active (t1 ≤ t < t2)

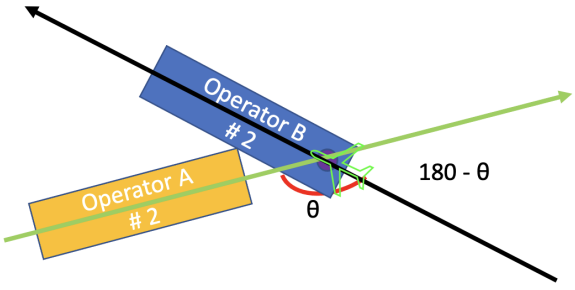

(b) Next, operational volume blocks # 2 of UAS operators are active (t2 ≤ t < t3)

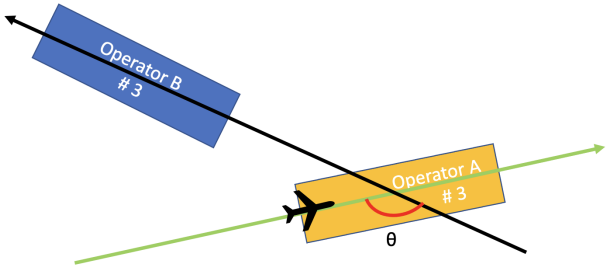

(c) Finally, operational volume blocks # 3 of UAS operators are active (t3 ≤ t < t4)

Fig. 3 Case Study I - Incoming Crossing at Obtuse Angle

is as follows:

$$\Delta T_{UA-OVB} = \Delta T_{OVB-OVB} + \frac{d_{TE-WPT}}{V_A} = \frac{2l_B}{V_B} + \frac{W_B}{2V_A \sin\theta} - \frac{W_A \cos\theta}{2V_A \sin\theta} \tag{2}$$

where the different terms used in Equation 1 and Equation 2 are defined in Table 1.

2. Case Study II - Incoming Crossing at Obtuse Angle (90 deg < θ < 180 deg)

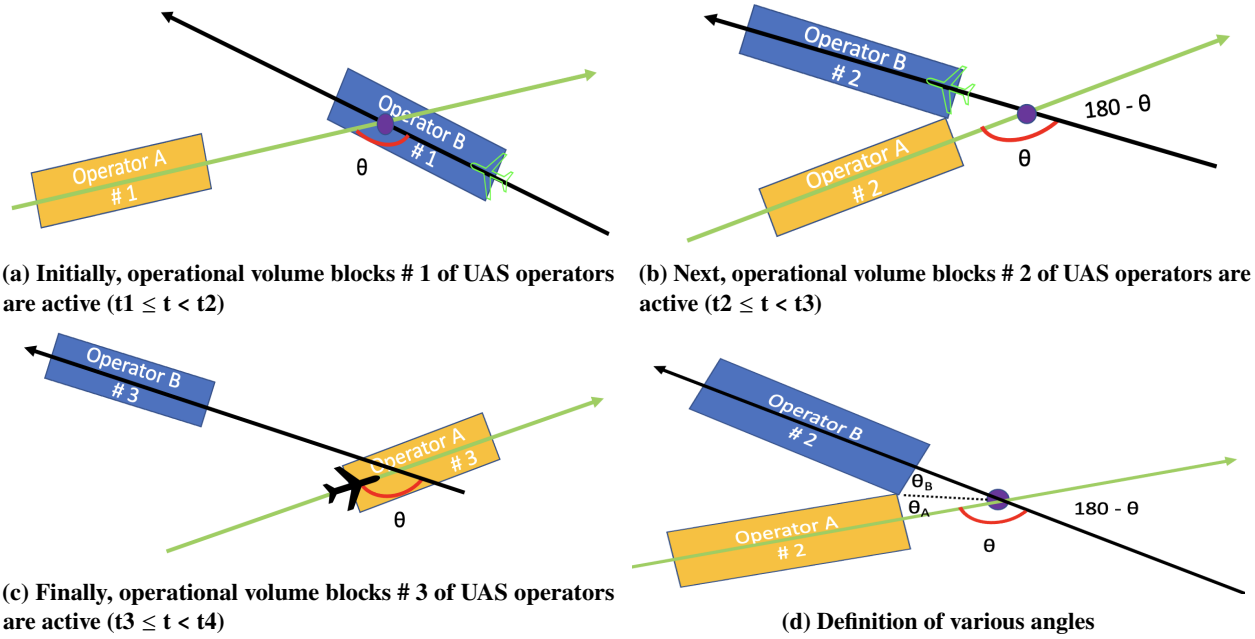

(a) Initially, operational volume blocks # 1 of UAS operators are active (t1 ≤ t < t2)

(b) Next, operational volume blocks # 2 of UAS operators are active (t2 ≤ t < t3)

(c) Finally, operational volume blocks # 3 of UAS operators are active (t3 ≤ t < t4)

(d) Definition of various angles

Fig. 4 Case Study II - Incoming Crossing at Obtuse Angle

As shown in Subfigure 4a active operational volume block (# 1) of UAS operator B has enclosed the crossing waypoint such that the active operational volume block (# 1) of UAS operator A can not enclose the crossing waypoint. Similarly, as shown in Subfigure 4b, since the active operational volume block (# 2) of UAS operator B has the trailing edge blocking the crossing waypoint, therefore, the active operational volume block (# 2) of UAS operator A can not enclose the crossing waypoint. In this case study, the point on the leading edge of UAS operator A's operational volume block (# 2) touches the trailing edge of UAS operator B's operational volume block (# 2). Hence once the operational volume block (# 2) of UAS operator B deactivates, the operational volume block (# 3) of UAS operator A can enclose the crossing waypoint as shown in Subfigure 4c. The temporal separation at the crossing waypoint for strategic deconfliction of active operational volume blocks of UAS operators A and B is as follows:

$$\Delta T_{OVB-OVB} = \frac{2l_B}{V_B} \tag{3}$$

Temporal separation between the estimated time of arrival of the UA of UAS operator A at the crossing waypoint and the activation time of the first active operational volume block (# 1) of UAS operator B blocking the crossing waypoint can be calculated by solving the following equations:

$$\frac{W_A}{\sin\theta_A} = \frac{W_B}{\sin\theta_B} \tag{4}$$

$$\theta_A + \theta_B = 180 - \theta \tag{5}$$

$$\Delta T_{UA-OVB} = \Delta T_{OVB-OVB} + \frac{d_{TE-WPT}}{V_A} = \frac{2l_B}{V_B} + \frac{W_A}{2V_A \tan\theta_A} \tag{6}$$

where the different terms used in Equation 3 to Equation 6 are defined in Table 1 and shown in Subfigure 4d.

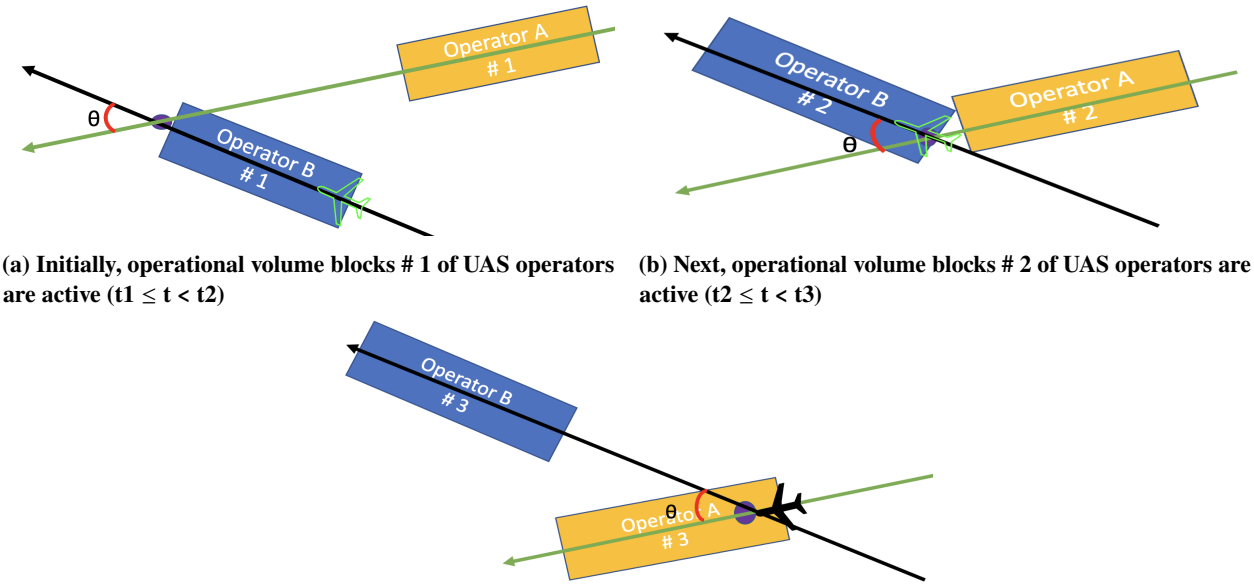

(a) Initially, operational volume blocks # 1 of UAS operators are active (t1 ≤ t < t2)

(b) Next, operational volume blocks # 2 of UAS operators are active (t2 ≤ t < t3)

(c) Finally, operational volume blocks # 3 of UAS operators are active (t3 ≤ t < t4)

Fig. 5 Case Study III - Incoming Crossing at Acute Angle

3. Case Study III - Incoming Crossing at Acute Angle (0 deg < θ < 90 deg)

As shown in Subfigure 5a active operational volume block (# 1) of UAS operator B has enclosed the crossing waypoint such that the active operational volume block (# 1) of UAS operator A can not enclose the crossing waypoint. Similarly, as shown in Subfigure 5b, since the active operational volume block (# 2) of UAS operator B has the trailing edge blocking the crossing waypoint, therefore, the active operational volume block (# 2) of UAS operator A can not enclose the crossing waypoint. In this case study, the point on the leading edge of UAS operator A's operational volume block (# 2) touches the trailing edge of UAS operator B's operational volume block (# 2).Hence once the operational volume block (# 2) of UAS operator B deactivates, the operational volume block (# 3) of UAS operator A can enclose the crossing waypoint as shown in Subfigure 5c. The temporal separation at the crossing waypoint for strategic deconfliction of active operational volume blocks of UAS operators A and B is as follows:

$$\Delta T_{OVB-OVB} = \frac{2l_B}{V_B} \tag{7}$$

Temporal separation between the estimated time of arrival of the UA of UAS operator A at the crossing waypoint and the activation time of the first active operational volume block (# 1) of UAS operator B blocking the crossing waypoint is as follows:

$$\Delta T_{UA-OVB} = \Delta T_{OVB-OVB} + \frac{d_{TE-WPT}}{V_A} = \frac{2l_B}{V_B} + \frac{W_B \sin\theta}{2V_A} \tag{8}$$

where the different terms used in Equation 3 to Equation 8 are defined in Table 1.

4. Case Study IV - Incoming Crossing at Acute Angle (0 deg < θ < 90 deg)

As shown in Subfigure 6a active operational volume block (# 1) of UAS operator B has enclosed the crossing waypoint such that the active operational volume block (# 1) of UAS operator A can not enclose the crossing waypoint. In this case study, the point on the leading edge of UAS operator A's operational volume block (# 2) touches the trailing edge of UAS operator B's operational volume block (# 2). However, once the operational volume block (# 1) of UAS operator B deactivates, the operational volume block (# 2) of UAS operator A can enclose the crossing waypoint as shown in Subfigure 6b. The temporal separation at the crossing waypoint for strategic deconfliction of active operational volume blocks of UAS operators A and B is as follows:

$$\Delta T_{OVB-OVB} = \frac{l_B}{V_B} \tag{9}$$

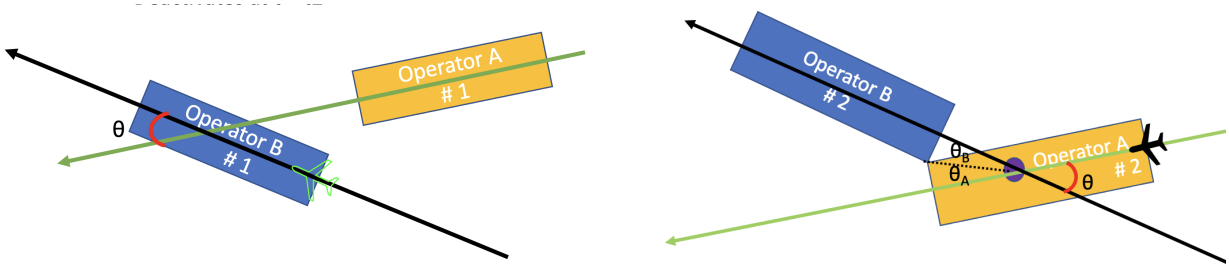

(a) Initially, operational volume blocks # 1 of UAS operators are active (t1 ≤ t < t2)

(b) Finally, operational volume blocks # 2 of UAS operators are active (t2 ≤ t < t3)

Fig. 6 Case Study IV - Incoming Crossing at Acute Angle

Temporal separation between the estimated time of arrival of the UA of UAS operator A at the crossing waypoint and the activation time of the first active operational volume block (# 1) of UAS operator B blocking the crossing waypoint can be calculated by solving the following equations:

$$\frac{W_A}{\sin\theta_A} = \frac{W_B}{\sin\theta_B} \tag{10}$$

$$\theta_A + \theta_B = \theta \tag{11}$$

$$\Delta T_{UA-OVB} = \Delta T_{OVB-OVB} + \frac{d_{TE-WPT}}{V_A} = \frac{l_B}{V_B} + \frac{l_A}{V_A} - \frac{W_A}{2V_A \tan\theta_A} \tag{12}$$

where the different terms used in Equation 9 to Equation 12 are defined in Table 1 and shown in Subfigure 6b.

B. Discussions on Analytical Case Studies

From the four analytical case studies (Equations 1 to 12) involving two obtuse and two acute incoming crossing angles, the following observations can be made for strategic deconfliction at crossing waypoints:

- Minimum temporal separation between active operational volume blocks of two different UAS operators at a crossing waypoint to avoid spatiotemporal overlapping (Equations 1, 3, 7, and 9):
  - is directly proportional to the transit time of the UA (sequencing the waypoint first) in the active operational volume block, therefore,
    - directly proportional to the length of operational volume blocks (enclosing the crossing waypoint).
    - inversely proportional to the groundspeed of UA sequencing the crossing waypoint first.
  - in most cases, it only depends on the length of operational volume blocks and groundspeed of the unmanned aircraft sequencing the crossing waypoint first.
- Minimum temporal separation between the UA (sequencing second) and operational volume blocks of the UA (sequencing the waypoint first) at a crossing waypoint to avoid spatiotemporal overlapping (Equations 2, 6, 8, and 12) is:
  - is directly proportional to the transit time of the UA (sequencing the waypoint first) in the active operational volume block, therefore,
    - directly proportional to the length of operational volume blocks (enclosing the crossing waypoint).
    - inversely proportional to the groundspeed of UA sequencing the crossing waypoint first.
  - a nonlinear function of the width of operational volume blocks and incoming crossing angle that depends on the two unmanned aircraft's relative positions of operational volume blocks.

III. Simulation Studies of Strategic Deconfliction at Crossing Waypoints

In the simulation case studies, two depot locations are considered as departure ports for UA (UAVs) of UAS operators A and B (shown in Table 2). The UAS departure traffic at both depots is simulated using a Poisson distribution with an on-demand service request rate, as shown in Table 3. The Poisson distribution has been used to model the on-demand service request at two depots because each demand request is assumed to be discrete, independent, and mutually exclusive, but at an average rate (λ) when viewed as a group for a set of demands. Two different routes are

considered per depot, so lateral paths have incoming crossing angles of 35 deg and 135 deg, respectively. However, each scenario has one route per depot, as shown in Subfigure 7a. The 4D trajectory of a UA is computed using flight kinematics, flight dynamics, UA performance data, and path constraints from [12] as shown in Subfigure 7b.

Table 2 Depot Locations

Depot	Latitude (deg)	Longitude (deg)
UAS Operator A	37.40089	-122.10945
UAS Operator B	37.46609	-122.13675

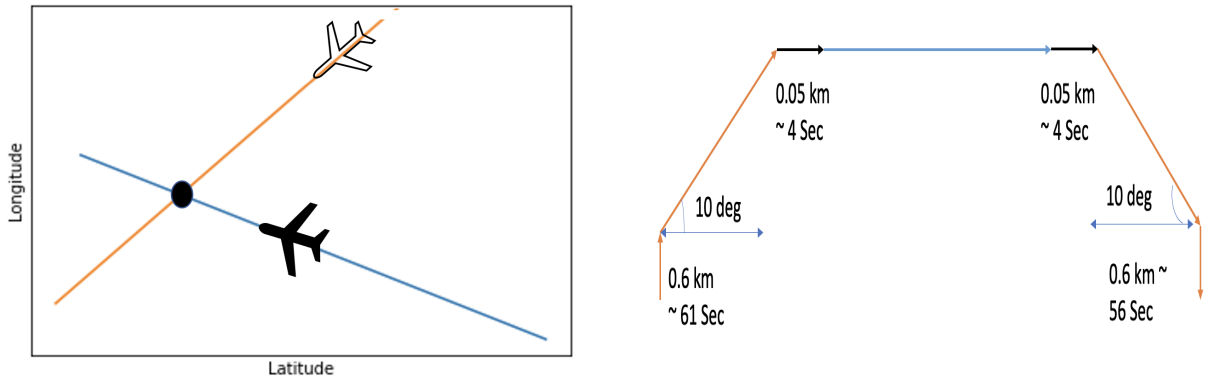

(a) Illustration of lateral paths crossing at a waypoint **(b) Vertical profile of an UA**

Fig. 7 Illustration of Lateral and Vertical Profiles of Unmanned Aircraft

A. Strategic Deconfliction Using Linear Programming Approach

The strategic deconfliction of UA (UAVs) at a crossing waypoint, depot A (departure port), and depot B (departure port) has been formulated as a linear programming problem because the objective function, i.e., average ground delay and all the temporal constraints on UA are linear for a given crossing angle, minimum departure separation and operational volume blocks length and width. The minimum temporal separation between UA of different UAS operators at a crossing waypoint has been imposed based on temporal separation equations derived in Section II.A for strategic deconfliction. The linear programming problem is then solved for an optimized solution using Gurobi [13]. The strategic deconfliction at departure ports and the crossing waypoint is performed by adding delays to the departure time of UAs. Therefore, for each scenario, the flight duration of a UA to the crossing waypoint from a depot remains constant, and adjustment to the arrival time at the crossing waypoint is performed by adjustment in the departure time of a UA.

1. Objective Function

In this research, the objective function of the linear programming problem is the average ground (per individual UA) due to potential spatiotemporal conflict between operational volume blocks of a UAS operator with the UA of another UAS operator at the crossing waypoint of UAVs scheduled to depart from depot A and depot B. Therefore, the average ground delay (per individual UA) is defined as:

$$\text{Minimize} \quad \frac{\sum_{i=0}^{n_A} \text{GD}_\text{i} + \sum_{j=0}^{n_B} \text{GD}_\text{j}}{n_A + n_B} \tag{13}$$

where GD_i and GD_j are the ground delays of the i^{th} UA of the UAS operator A, and j^{th} UA of the UAS operator B, respectively. Here, n_A and n_B are the total numbers of flights scheduled to depart from depot A and depot B, respectively.

2. Minimum Temporal Separation at Departure Ports

The on-demand service request to deliver packages using UA (UAVs) at each depot is simulated using a Poisson distribution. The scheduled time of departure (STD) of each UA is separated from its on-demand service request time (ODT) by a flight preparation time ($\Delta t_{\text{Flight Preparation}}$) at each departure port:

$$\text{STD(i)} \geq \text{ODT(i)} + \Delta t_{\text{Flight Preparation}} \tag{14}$$

where ODT(i) is the on-demand service request time for the i^{th} UA, STD(i) is the scheduled time of departure for the i^{th} UA, and flight preparation time ($\Delta t_{\text{Flight Preparation}}$) is the time required for the UA flight preparation (on-demand order processing, packaging of order, loading of delivery package to the assigned UA, and pre-flight checks).

At the departure port of UAS operator A and UAS operator B, scheduled time of departure (STD) of two consecutive UA (UAVs) are separated by at least the minimum departure time separation ($\Delta t_{\text{Departure Port}}$):

$$\text{STD(i+1)} \geq \text{STD(i)} + \Delta t_{\text{Departure Port}} \tag{15}$$

3. Minimum Temporal Separation at a Crossing Waypoint

The minimum temporal separation ($\Delta t_{\text{Crossing Waypoint}}$) constraint between two UA (UAVs) of different UAS operators at the crossing waypoint is as follows:

$$\text{RTA(j)} - \text{RTA(i)} \geq \Delta t_{\text{Crossing Waypoint}} \quad \forall\ \text{ETA(j)} > \text{ETA(i)} \tag{16}$$

where RTA(i) is the required time of arrival, ETA(i) is the earliest estimated time of arrival of the i^{th} UA of a UAS operator to the crossing waypoint, and RTA(j) is the required time of arrival to the crossing waypoint, ETA(j) is the earliest estimated time of arrival of the j^{th} UA of the other UAS operator to the crossing waypoint.

The required time of arrival (RTA) of a UA to the crossing waypoint is as follow:

$$\text{RTA(i)} = \text{STD(i)} + \text{FD(i)} \tag{17}$$

where FD(i) is the flight duration of the i^{th} flight to the crossing waypoint.

In this research, using a conservative approach, the minimum temporal separation at a crossing waypoint is defined using equations for calculating ΔT_{UA-OVB} in Section II. A UAS operator is assumed to not have real-time position and velocity information of a UA of another UAS operator. However, the UAS operator would have real-time position and active time information about an active operational volume block of another UAS operator.

- For an incoming crossing angle > 90 deg (obtuse angle), the minimum temporal separation ($\Delta t_{\text{Crossing Waypoint}}$) at the crossing angle is defined using equations 2 and 6 from Section II.A as follows:

$$\Delta t_{\text{Crossing Waypoint}} = \max\left(\frac{2l_B}{V_B} + \frac{W_B}{2V_A \sin\theta} - \frac{W_A \cos\theta}{2V_A \sin\theta}\ ,\ \frac{2l_B}{V_B} + \frac{W_A}{2V_A \tan\theta_A}\right) \tag{18}$$

- For an incoming crossing angle < 90 deg (acute angle), the minimum temporal separation ($\Delta t_{\text{Crossing Waypoint}}$) at the crossing angle is defined using equations 8 and 12 from Section II.A as follows:

$$\Delta t_{\text{Crossing Waypoint}} = \max\left(\frac{2l_B}{V_B} + \frac{W_B \sin\theta}{2V_A}\ ,\ \frac{l_B}{V_B} + \frac{l_A}{V_A} - \frac{W_A}{2V_A \tan\theta_A}\right) \tag{19}$$

B. Parametric Study on Minimum Temporal Separation

Figure 8 shows the minimum temporal separation as a function of the length [0, 100 m, ..., 1000 m] of the operational volume blocks using equations 18 and 19 for two different crossing angles (35 deg and 135 deg), four different widths of the operational volume blocks (50 m, 200 m, 350 m, and 500 m) and UA (UAVs) flying at cruise groundspeed of 20 m/s. From Figure 8, it can be seen that impact of the incoming crossing angle on the minimum temporal separation at a crossing waypoint increases with an increase in the width of the operational volume blocks.

C. Simulation Results and Discussions

The demand for each package delivery at a depot (A or B) is anticipated to be at random time because of the on-demand nature of UAS package delivery, but at an average rate (λ) when viewed as a group for a set of demands. Therefore, package delivery demand at each depot has been simulated using the Poisson distribution process [14]. In this research, each simulation run contains a fixed number of UAS flights from each depot (A and B).

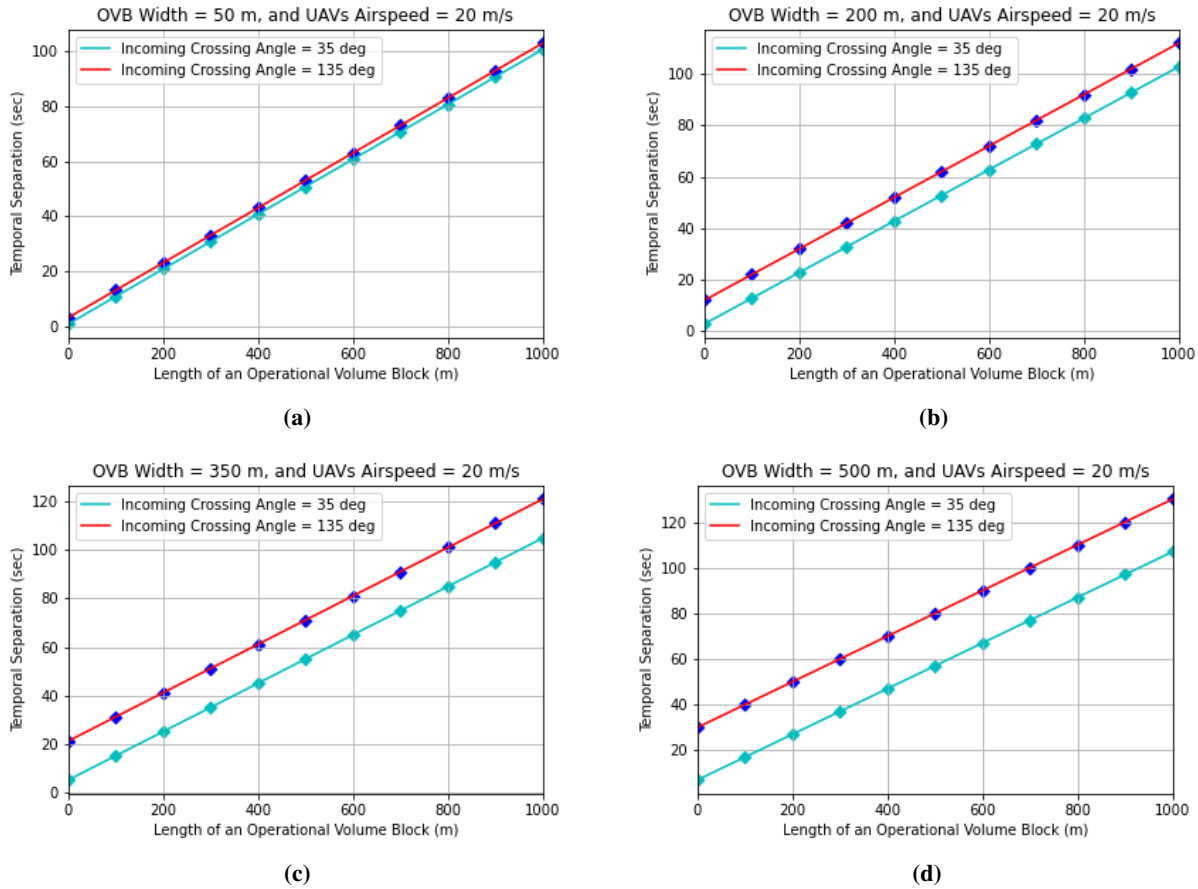

Fig. 8 Variation in Minimum Temporal Separation as a Function of Length and Width of Operational Volume Blocks

1. Simulation Study I

As shown in Table 3, various parameters have been varied to understand their impact on the ground delay of the group of UAS flights. The average ground delay of the group of UAS flights scheduled to takeoff from depot A and depot B has been used as a metric to study the impact mentioned above. For a given incoming crossing angle (35 deg or 135 deg) of two routes, minimum departure time separation ($\Delta t_{\text{Departure Port}}$) and on-demand departure rate (λ), traffic is generated using Poisson distribution for 10 different instances as shown in Figure 9. From Figure 9, it can be seen that:

- the impact of the minimum temporal separation at a crossing waypoint on the ground delay of flights is negligible if the minimum departure time separation ($\Delta t_{\text{Departure Port}}$) is at least twice the minimum temporal separation. This is because when the minimum departure time separation ($\Delta t_{\text{Departure Port}}$) at both depots is two times the minimum temporal separation ($\Delta t_{\text{Crossing Waypoint}}$), then both streams can be synced such that at the crossing waypoint, unmanned aircraft on the two routes arrive ($\Delta t_{\text{Crossing Waypoint}}$) apart.
- with an increase in minimum departure time separation ($\Delta t_{\text{Departure Port}}$) at a depot, the impact of increased length of operational volume blocks enclosing the crossing waypoint on the ground delay is offset to an extent. This observed behavior can be attributed to the fact that upon an increase in the minimum departure time separation ($\Delta t_{\text{Departure Port}}$), there is a larger time interval between flights, therefore less impact of the ground delay of one flight on another.

2. Simulation Study II

In this simulation study, as shown in Figure 10, number of flights per UAS operator and departure rate (λ) have been varied to understand their impact on the ground delay of the group of UAS flights. The average ground delay of UAS

Table 3 Parameters Relevant to Simulation Study I

Parameter	Value(s)
Incoming crossing angle	[35, 135] deg
$\Delta t_{\text{Flight Preparation}}$	3600 sec
Poisson demand rate λ	[1/60, 1/120] (1/sec)
$\Delta t_{\text{Departure Port}}$	[60, 120] sec
Length of operational volume blocks	[0, 100, ..., 1000] m
Width of operational volume blocks	50 m
Cruise groundspeed and cruise altitude MSL	20 m/s and 121 m (400 ft)
Number of flights per UAS operator	60

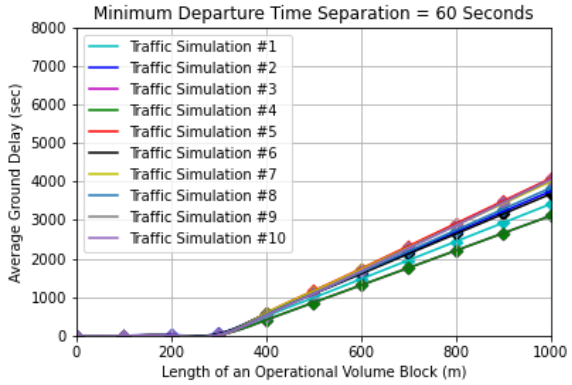

(a) Incoming crossing angle = 35 deg and departure rate (λ) = 1/60 (1/sec)

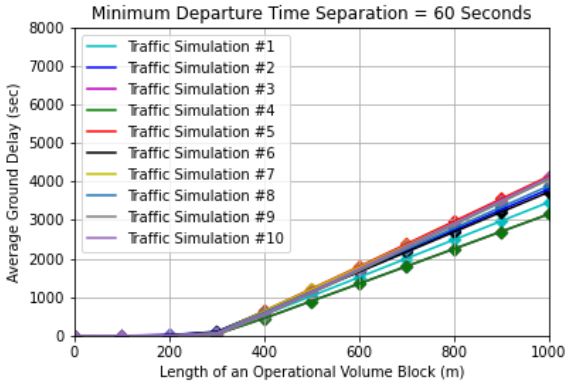

(b) Incoming crossing angle = 135 deg and departure rate (λ) = 1/60 (1/sec)

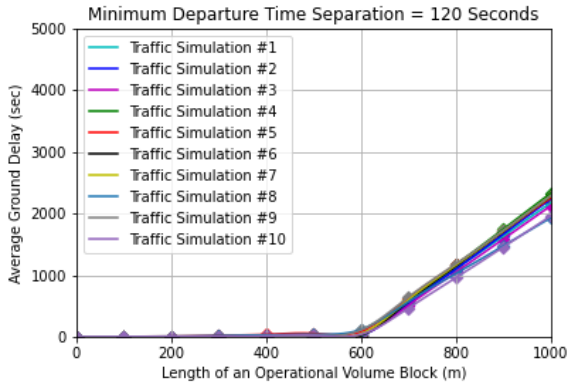

(c) Incoming crossing angle = 35 deg and departure rate (λ) = 1/120 (1/sec)

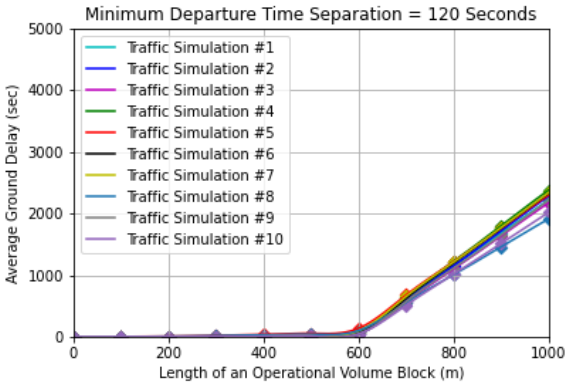

(d) Incoming crossing angle = 135 deg and departure rate (λ) = 1/120 (1/sec)

Fig. 9 Variation in Average Ground Delay of UAS Flights as a Function of Minimum Departure Time Separation, Departure Rate (λ), Length of the Operational Volume Block, and Incoming Crossing Angle

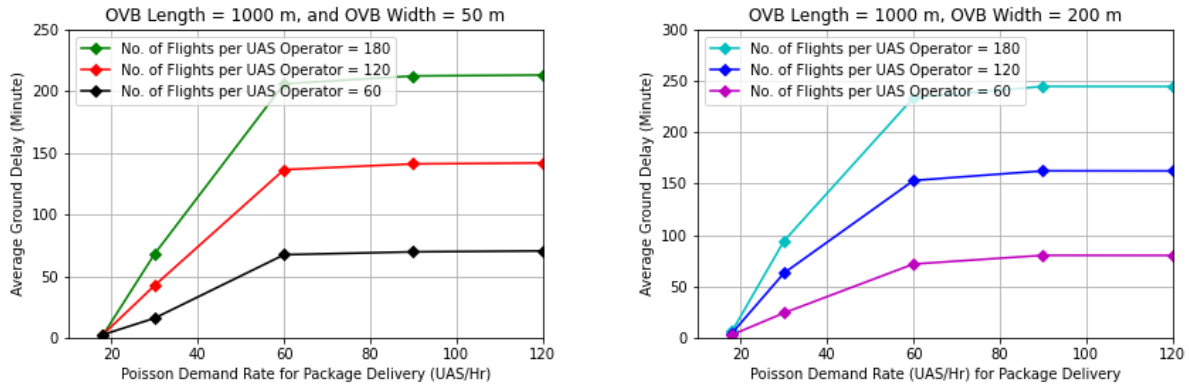

(a) **(b)**

Fig. 10 Variation in Average Ground Delay as a Function of Number of Flights per UAS Operator, Width of Operational Volume Blocks, and Poisson Demand / Departure Rate (λ) for 135 Deg Incoming Crossing Angle

flights has been used as a metric to study the impact mentioned above. In this simulation study, incoming crossing angle (θ = 135 deg) of two routes, operational volume blocks length (l = 1000 m) and minimum departure time separation ($\Delta t_{\text{Departure Port}}$ = 60 seconds) have been fixed, whereas on-demand departure rate (λ), operational volume blocks width and number of flights per UAS operator have been varied. The traffic for each scenario is generated using Poisson distribution as shown in Figure 10. From Figure 10, it can be seen that:

- with an increase in the number of flights per UAS operator, the average ground delay of overall UAS flights increases.
- once the on-demand departure rate (λ) is higher than the minimum departure time separation rate ($1/\Delta t_{\text{Departure Port}}$), the on-demand departure rate is clamped to ($1/\Delta t_{\text{Departure Port}}$), therefore, the average ground delay due to potential conflicts at the crossing waypoint remains constant with any further increase in the on-demand departure rate (λ).

IV. Conclusions

In this research, analytical case studies are first performed to understand the parameters on which the minimum temporal separation between unmanned aircraft at crossing waypoints is dependent for enabling strategic deconfliction. The analytical studies suggest that the minimum temporal separation between the unmanned aircraft (sequencing second) and operational volume blocks of the unmanned aircraft (sequencing the waypoint first) at a crossing waypoint to avoid spatiotemporal overlapping is:

- directly proportional to the transit time of the unmanned aircraft (sequencing the waypoint first) in the active operational volume block.
- a nonlinear function of the width of operational volume blocks and incoming crossing angle that depends on the two unmanned aircraft's relative positions of operational volume blocks.

Next, the parametric study shows that the impact of the incoming crossing angle on the minimum temporal separation at a crossing waypoint increases with an increase in the width of the operational volume blocks.

Finally, simulation studies are performed to understand the impact of operational volume block sizing, on-demand departure rate, minimum departure time separation, and the incoming crossing angle on the average ground delay of unmanned aircraft traveling on two routes with a single crossing waypoint and identical on-demand departure rate. Simulation study I suggests that:

- the impact of the minimum temporal separation at a crossing waypoint on the ground delay of flights is negligible if the minimum departure time separation ($\Delta t_{\text{Departure Port}}$) is at least two times the minimum temporal separation. This is because when the minimum departure time separation ($\Delta t_{\text{Departure Port}}$) at both depots is two times the minimum temporal separation ($\Delta t_{\text{Crossing Waypoint}}$), then both streams can be synced such that at the crossing waypoint, unmanned aircraft on the two routes arrive ($\Delta t_{\text{Crossing Waypoint}}$) apart.
- with an increase in minimum departure time separation ($\Delta t_{\text{Departure Port}}$) at a depot, the impact of increased length of operational volume blocks enclosing the crossing waypoint on the ground delay is offset to an extent. This

observed behavior can be attributed to the fact that upon an increase in the minimum departure time separation ($\Delta t_{\text{Departure Port}}$), there is a larger time interval between flights, therefore less impact on the ground delay of one flight on another.

Simulation study II suggests that:

- with an increase in the number of flights per operator, the average ground delay of overall flights increases for a given on-demand departure rate (λ) and minimum departure time separation at two depots.
- once the on-demand departure rate (λ) is higher than the minimum departure time separation rate ($1/\Delta t_{\text{Departure Port}}$), the on-demand departure rate is clamped to ($1/\Delta t_{\text{Departure Port}}$), therefore, the average ground delay due to the potential conflict at the crossing waypoint remains constant with any further increase in the on-demand departure rate (λ).

Acknowledgement

The material is partly based upon contractor work supported by NASA under award number NNA16BD14C for NASA Academic Mission Services (NAMS).

References

[1] Kopardekar, P., Rios, J., Prevot, T., Johnson, M., Jung, J., and Robinson, J. E., "Unmanned aircraft system traffic management (UTM) concept of operations," *AIAA Aviation and Aeronautics Forum (Aviation 2016)*, 2016.

[2] Federal Aviation Administration, "Advisory Circular: 107-2, Small Unmanned Aircraft Systems (sUAS)," , 2016. URL `www.faa.gov/documentlibrary/media/advisory_circular/ac_107-2.pdf`.

[3] "UTM ConOps Version2," *Federal Aviation Administration NextGen Office*, 2020. URL `https://www.faa.gov/uas/research_development/traffic_management/media/UTM_ConOps_v2.pdf`.

[4] Rios, J. L., Homola, J., Craven, N., Verma, P., and Baskaran, V., "Strategic Deconfliction Performance: Results and Analysis from the NASA UTM Technical Capability Level 4 Demonstration," 2020.

[5] Erzberger, H., Lauderdale, T., and Chu, Y., "Automated conflict resolution, arrival management, and weather avoidance for air traffic management," *Proceedings of the Institution of Mechanical Engineers, Part G: Journal of aerospace engineering*, Vol. 226, No. 8, 2012, pp. 930–949.

[6] Lauderdale, T. A., Pradeep, P., Edholm, K.-M., and Bosson, C. S., *Separation at Crossing Waypoints Under Wind Uncertainty in Urban Air Mobility*, 2021. https://doi.org/10.2514/6.2021-2351, URL https://arc.aiaa.org/doi/abs/10.2514/6.2021-2351.

[7] Verma, S. A., Monheim, S. C., Moolchandani, K. A., Pradeep, P., Cheng, A. W., Thipphavong, D. P., Dulchinos, V. L., Arneson, H., Lauderdale, T. A., Bosson, C. S., Mueller, E. R., and Wei, B., "Lessons Learned: Using UTM Paradigm for Urban Air Mobility Operations," *2020 AIAA/IEEE 39th Digital Avionics Systems Conference (DASC)*, 2020, pp. 1–10. https://doi.org/10.1109/DASC50938.2020.9256650.

[8] Kim, J., and Atkins, E., "Airspace Geofencing and Flight Planning for Low-Altitude, Urban, Small Unmanned Aircraft Systems," *Applied Sciences*, Vol. 12, No. 2, 2022, p. 576.

[9] Johnson, M., and Larrow, J., "UAS Traffic Management Conflict Management Model," 2020. URL https://www.nasa.gov/sites/default/files/atoms/files/2020-johnson-nasa-faa.pdf.

[10] Xue, M., and Do, M., "Scenario Complexity for Unmanned Aircraft System Traffic," *AIAA Aviation 2019 Forum*, 2019, p. 3513.

[11] Prevot, T., and Lee, P. U., "Trajectory-Based Complexity (TBX): A modified aircraft count to predict sector complexity during trajectory-based operations," *2011 IEEE/AIAA 30th Digital Avionics Systems Conference*, 2011, pp. 3A3–1–3A3–15. https://doi.org/10.1109/DASC.2011.6096045.

[12] Pradeep, P., Park, S. G., and Wei, P., "Trajectory optimization of multirotor agricultural UAVs," *2018 IEEE Aerospace Conference*, IEEE, 2018, pp. 1–7.

[13] Gurobi Optimization, LLC, "Gurobi Optimizer Reference Manual," , 2022. URL https://www.gurobi.com.

[14] Simaiakis, I., and Balakrishnan, H., "A queuing model of the airport departure process," *Transportation Science*, Vol. 50, No. 1, 2016, pp. 94–109.